ΣΥΝΕΔΡΙΑ ΤΗΣ 22ΑΣ ΝΟΕΜΒΡΙΟΥ 2001

ΠΡΟΕΔΡΙΑ ΝΙΚΟΛΑΟΥ ΚΟΝΟΜΗ

ΣΕΙΣΜΟΛΟΓΙΑ. — **Spatio-temporal complexity aspects on the interrelation between Seismic Electric Signals and Seismicity,** by *Panayiotis A. Varotsos, Nicholas V. Sarlis, Efthimios S. Skordas**, διὰ τοῦ Ἀκαδημαϊκοῦ κ. *Καίσαρος Ἀλεξοπούλου.*

ABSTRACT

Seismic Electric Signals (SES) are low frequency ($\leqslant 1$ Hz) changes of the electric field (E) of the earth that have been detected in Greece (*1, 2*) and Japan (*3*) and found to precede earthquakes with lead times ranging from several hours to a few months. Their analysis might well lead to an estimation of the epicentral area. Here we show that the spectral content of the seismicity in the area candidate to suffer an earthquake finally falls on the spectral content of the SES activity, just before the occurrence of the main shock. The key point is that both spectra have to be calculated in a new time domain, termed as «natural time», starting from the time of the SES recording. Thus, since the spectrum of the SES is known well in advance, the continuous inspection of the spectrum of the evolving seismic activity may lead to an estimation of the time window of the impending main shock with an accuracy of around a few days.

Recent laboratory measurements (*4*) showed that, as the glass transition is approached, a polarisation time series is emitted which arises from the reorientation process of electric dipoles; this process includes a large number of atoms (cooperativity) (*4*). The feature of these series is strikingly similar

* Π. ΒΑΡΩΤΣΟΥ, Ν. ΣΑΡΛΗ καὶ Ε. ΣΚΟΡΔΑ, **Προτάσεις χωρο-χρονικῆς πολυπλοκότητας γιὰ τὴν συσχέτιση μεταξὺ Σεισμικῶν Ἠλεκτρικῶν Σημάτων καὶ Σεισμικότητας.**

(*5*) to the Seismic Electric Signals (SES) activities; examples of the latter are shown in Fig. 1a (see also Table 1). This similarity is reminiscent of the pressure stimulated currents SES generation model (*6*), which suggests that SES are emitted due to the (re)orientation of electric dipoles when reaching a critical pressure (stress) P_{cr}. It was also argued that the (re)orientation process of each electric dipole (see p. 404 of Ref. *6*) has a migration volume, v^m, orders of magnitude larger than the mean atomic volume. Thus, the aforementioned laboratory measurements fortify the suggestion (*5, 7*) that the emission of the SES activities could be discussed in the frame of the theory of *dynamic phase transitions.*

Here we show that an interrelation exists between the time evolution of the seismic activity (measured from the start of the SES recording) and the spectrum characteristics of the SES. This, however, can be only achieved if we depart from the conventional time t and think in terms of a *natural time* χ. The latter serves as an index for the occurrence of an event (reduced by the total number of events, thus being smaller than, or equal to, unity). Let us, therefore, denote by Q_k the duration of the k^{th} transient pulse (single SES) of an SES activity comprised of N pulses (Fig. 1A). The natural time χ is introduced by ascribing to this pulse the value $\chi_k = k/N$. If we now consider the evolution (χ_k, Q_k), we can define the continuous function $F(\omega)$ (this should not be confused with the discrete Fourier transform):

$$F(\omega) = \sum_{k=1}^{N} Q_k \exp\left(i\omega \frac{k}{N}\right)$$

where $\omega = 2\pi\phi$, and ϕ stands for the *natural frequency.* We normalize $F(\omega)$ by dividing it by $F(0)$

$$\Phi(\omega) = \frac{\sum_{k=1}^{N} Q_k \exp\left(i\omega \frac{k}{N}\right)}{\sum_{k=1}^{N} Q_k} = \sum_{k=1}^{N} p_k \exp\left(i\omega \frac{k}{N}\right) \qquad [1]$$

where $p_k = Q_k \Big/ \sum_{n=1}^{N} Q_n$. Thus, the quantities p_k describe a «probability» to observe the transient at natural time χ_k. From Eq. (1), we can obtain the normalized power spectrum $\Pi(\omega)$:

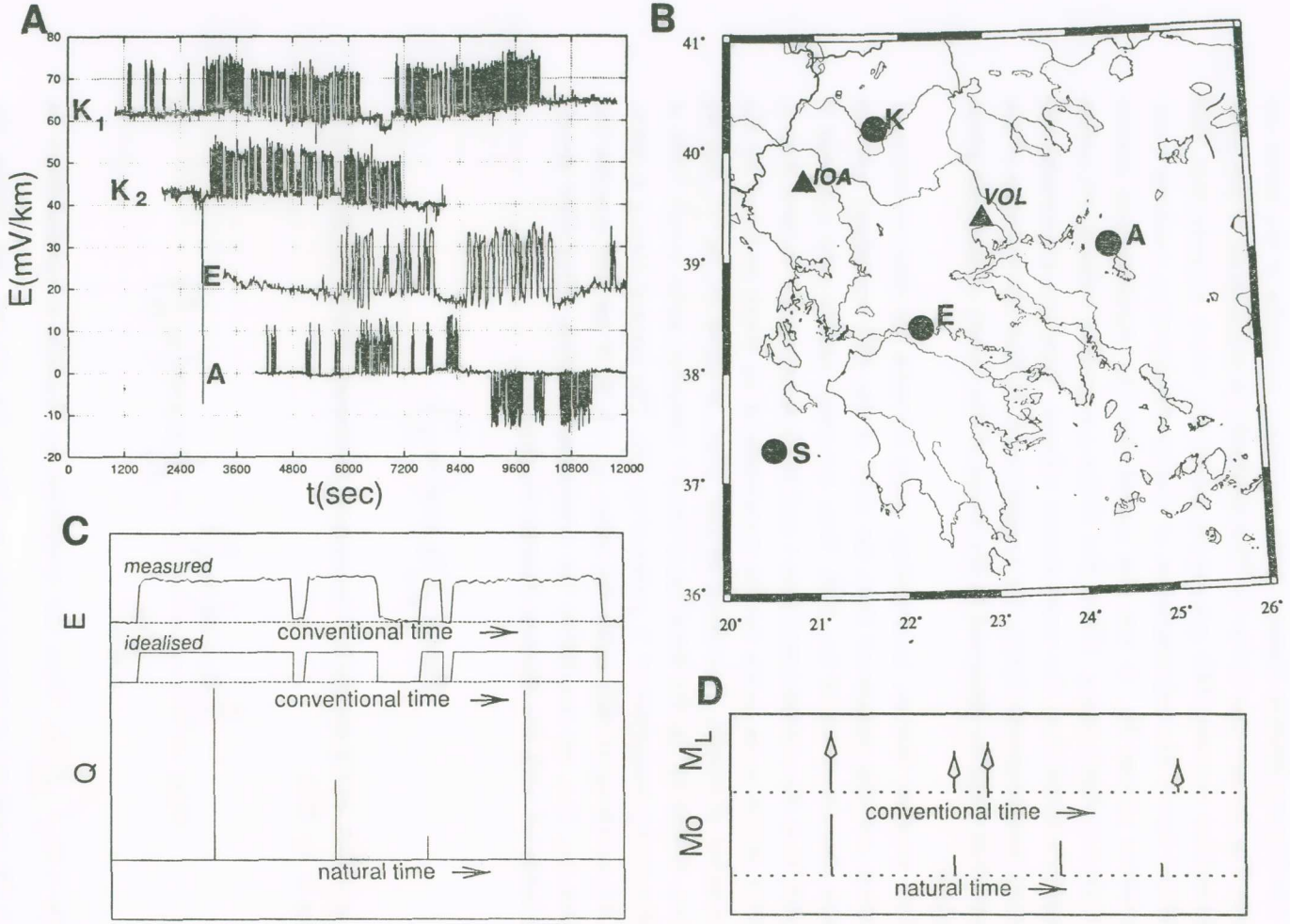

Fig. 1. (a) SES activities recorded before the main shocks K, E, S and A given in table 1; K_1 and K_2 refer to the two SES activities before the EQ labeled K. The upper two SES activities were recorded at IOA, while the lower two ones at VOL. (b) Map showing the EQ epicenters (cycles) and the sites (triangles) of the measuring SES stations. How a series of electric pulses (c) or a series of seismic events (d) can be read in «natural time». In both cases the natural time serves as an index of the occurrence of each event (reduced by the total number of events), while the amplitude is proportional to (c) the duration of each electric pulse and (d) to the seismic moment M_0.

TABLE 1.

All EQS with MS(USGS) $\geqslant$ 6.0 within $N_{36.5}^{41.5}$ $E_{19.0}^{26.0}$ and the relevant SES activities.

Main Earthquakes					SES activities*				Region Considered
EQ label	Date	Time	Epicenter	MS (USGS)	Date	Time	Station	Reference	Coordinates
K	13-05-1995	08 : 47	40.2N - 21.7E	6.6	18&19-04-1995	10 : 04	IOA	(*2*)	$N_{39.2}^{40.5}$ $E_{20.3}^{22.0}$
E	15-06-1995	00 : 15	38.4N - 22.2E	6.5	30-04-1995	05 : 41	VOL	(*2*)	$N_{37.5}^{39.7}$ $E_{21.5}^{25.0}$
S	18-11-1997	13 : 07	37.3N - 20.5E	6.4	03-10-1997	18 : 24	IOA	(*11*)	$N_{37.0}^{38.5}$ $E_{20.3}^{21.7}$
A	26-07-2001	00 : 21	39.1N - 24.4E	6.6	17-03-2001	15 : 34	VOL	(*12*)	$N_{38.7}^{39.5}$ $E_{22.0}^{25.0}$

* Data collected with 1 sample/sec (except of case E in which the rate was 1 sample/10 sec).

$$\Pi(\omega) = |\Phi(\omega)|^2 \qquad [2]$$

For natural frequencies ϕ less than 0.5, $\Pi(\omega)$ or $\Pi(\phi)$ reduce to a characteristic function for the probability distribution p_k in the context of probability theory. The procedure of reading a series of electric pulses in the natural time domain is depicted in Fig. 1C. The evolution of the seismic activity should be considered in the same framework by ascribing to the k^{th} event, instead of Q_k, the corresponding seismic moment M_0 (Fig. 1D). In what follows, we apply this procedure to the data related to the four strongest earthquakes (EQ)s (labelled K, E, S and A, Table 1 and Fig. 1B) that occurred in Greece since 1988.

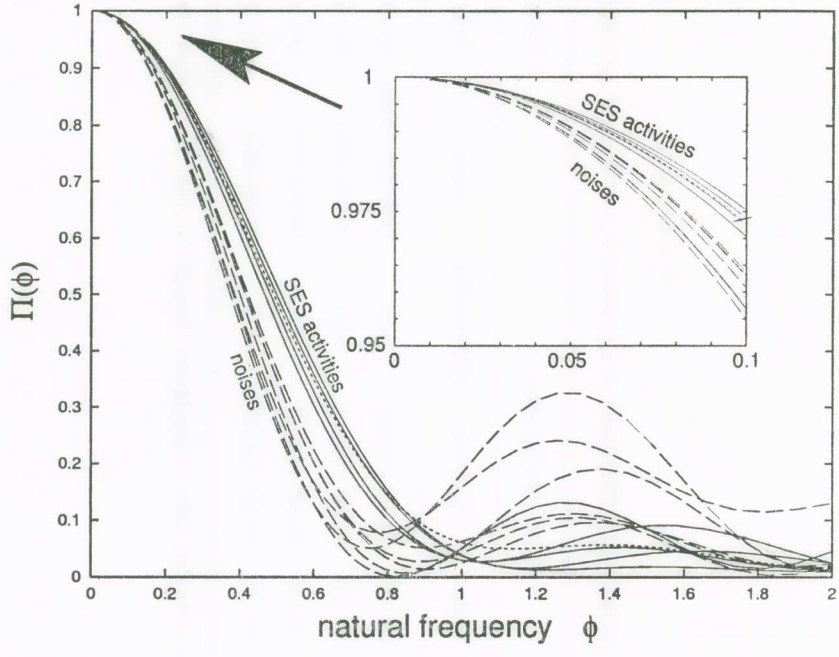

Fig. 2. The normalised power spectra $\Pi(\phi)$ for the SES activities (solid lines) related with the EQs labeled: K, E and A (from the top to the bottom: K_1, A, E, K_2) along with those of a number of artificial noises (broken lines). The dotted curve corresponds to a theoretical estimation emerged from the theory of critical phenomena.

We first start with the analysis of the SES activities. Once an SES activity has been recorded, we can read it in the natural time domain and then proceed to its analysis. Figure 2 depicts, as an example, $\Pi(\phi)$ for the SES acti-

vities, along with a number of artificial noises which have a similar feature with SES. An inspection of this figure shows the following three facts: First, the curves fall practically into two different classes, labelled «noises» and «SES activities» respectively. This classification, which might be theoretically understood (see the appendix), provides a tool for a distinction between noises and SES. Such a distinction can be alternatively made, e.g., by ensuring that the electric field variations precede (*8*) the associated variations of the magnetic field by a lead time of the order of 1 sec for epicentral distances of around 100 km. Secondly, Fig. 2 reveals that, for *natural frequencies* smaller than 0.5, the corresponding $\Pi(\phi)$ values of the SES activities scatter around the dotted curve, which has been estimated from theoretical considerations when approaching a critical point (see the appendix). Thirdly, the curves related to the SES activities crossa at point with a ϕ value very close to unity, i.e., $\phi \approx 1.05$. How this point is approached can be studied by means of the so-called *β-function* (see p. 288 of Ref. *9*) when following a procedure similar to that developed in Ref. *10*.

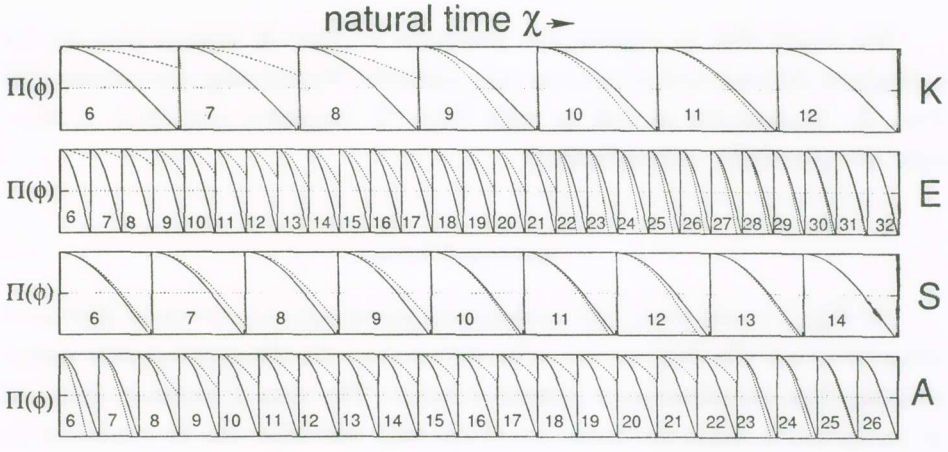

Fig. 3. Time evolution of the normalised power spectra $\Pi(\phi)$, in the window $0<\phi\leqslant 0.5$, of the seismic activities (broken line) along with those obtained for the SES activities (solid lines) for the cases of the strong EQS labeled K, E, S and A. The numbers refer to the last event considered in order to calculate the seismicity spectrum (and correspond to the events reported in the tables of the appendix). For the SES activities K_1, K_2, their average is used while for S the theoretical estimation (Fig. 2) is plotted.

We now turn to a study of the interrelation of the natural spectra of the SES activities and the evolution of the subsequent seismic activities. The continuous lines in Fig. 3 depict the normalised power spectra, $\Pi(\phi)$, deduced from the analysis of the SES activities. In the same figure, we plot (broken lines) the corresponding quantity $\Pi(\phi)$ obtained from the seismic activity for each case (of the four strong EQs mentioned earlier), as it evolves *after* the SES detection, event after event (see the appendix). A careful inspection of this figure shows that the broken lines fall on the continuous line *a few days* before the main shock-*at the most.* We emphasise that this occurs only if we consider the totality of the SES activity, and we do not, e.g., omit a significant portion of its initiation; and this in spite of the fact that, in the aforementioned four strong EQs, the corresponding lead times have a large diversity (lying between three weeks and 3.5 months; Table 1).

The suggestions in this work open up the possibility of estimating the time of the impending event with accuracy appreciably better than hitherto available.

ACKNOWLEDGEMENTS

We would like to express our gratitude to Prof. K. Alexopoulos for his continuous interest and advices on this research. Stimulating discussions with Prof. E. Manousakis as well as with Prof. N. Antoniou and Prof. C. Ktoridis are gratefully acknowledged.

APPENDIX

In Fig. 2 (main text), the normalized power spectra curves of SES activities lie above the $\Pi(\phi)$ curves related to noises. An attempt towards understanding this classification is presented below. The case of noises is discussed in paragraph I, while the behavior of the SES activities can be explained by using aspects of the theory of critical phenomena developed in paragraph II. Finally in paragraph III we present aspects on the normalized «natural» power spectrum for seismicity.

I. The normalised «natural» power spectrum $\Pi(\varphi)$ of noises

The Taylor expansion of Eq. (2) using Eq. (1) (main text) reveals that

$$\Pi(\omega) = 1 - \varkappa_1\omega^2 + \varkappa_2\omega^4 + \varkappa_3\omega^6 + \varkappa_4\omega^8 + \ldots \qquad [A.1]$$

where

$$\varkappa_1 = \langle\chi^2\rangle - \langle\chi\rangle^2 \qquad [A.2]$$

s the variance of χ,

$$\varkappa_2 = \frac{\langle\chi^2\rangle^2}{4} + \frac{\langle\chi^4\rangle}{12} - \frac{\langle\chi\rangle\langle\chi^3\rangle}{3} \qquad [A.3]$$

$$\varkappa_3 = \frac{\langle\chi^3\rangle^2}{36} + \frac{\langle\chi\rangle\langle\chi^5\rangle}{60} - \frac{\langle\chi^6\rangle}{360} - \frac{\langle\chi^2\rangle\langle\chi^4\rangle}{24} \qquad [A.4]$$

$$\varkappa_4 = \frac{\langle\chi^8\rangle}{20160} + \frac{\langle\chi^2\rangle\langle\chi^6\rangle}{720} + \frac{\langle\chi^4\rangle^2}{576} - \frac{\langle\chi^3\rangle\langle\chi^5\rangle}{360} - \frac{\langle\chi\rangle\langle\chi^7\rangle}{2520} \qquad [A.5]$$

and

$$\langle\chi^n\rangle = \sum_{k=1}^{N} (\chi_k)^n p_k \qquad [A.6]$$

are the moments of the distribution of χ.

The most useful quantity around $\omega = 0$, is the variance $\varkappa_1$ of the natural time distribution. This is so, because the various normalized power spectra are grouped together as ω or ϕ tend to 0 depending on their $\varkappa_1$ values. The value of the variance $\varkappa_1$ that reproduces noises is larger than 0.084, while for the SES activities the $\varkappa_1$ value is around 0.07.

In the limit of N tending to infinity, the distribution of p_k values will be substituted by a continuous probability density frunction $p(\chi)$ for $\chi \in (0, 1]$. In this region, $p(\chi)$ can be expanded in a cosine Fourier series

$$p(\chi) = 1 + \sum_{n=1}^{\infty} p_n \cos(n\pi\chi) \qquad [A.7]$$

where

$$p_n = 2\int_0^1 p(\chi)\cos(n\pi\chi)d\chi \qquad [A.8]$$

are the Fourier expansion coefficients.

Equation (A.7) could give insight into what one should expect for the normalized power spectra $\Pi(\omega)$. We recall that the lowest frequency included in this expansion, in addition to $\phi = 0$, is $\phi = 0.5$ that corresponding to $\omega_1 = 1\pi$; furthermore, recall that $\Pi(\omega)$ for $\phi < 0.5$ becomes a characteristic function for $p(\chi)$.

The following interrelation between the value of $\varkappa_1$ with the Fourier expansion coefficients of $p(\chi)$ can be found

$$\varkappa_1 = \langle\chi^2\rangle - \langle\chi\rangle^2 = \frac{1}{12} + \frac{1}{2\pi^2}\sum_{k=1}^{\infty}\frac{p_{2k}}{k^2} - \left(\frac{1}{2\pi^2}\sum_{k=0}^{\infty}\frac{p_{2k+1}}{\left(k+\frac{1}{2}\right)^2}\right)^2 \qquad [A.9]$$

We now calculate the limit for the variance $\varkappa_1$ in the case of a uniform distribution. When all the p_k are zero, we obtain the value of $\varkappa_1 = 1/12 = 0.0833...$ This, in the case of our experimental results, corresponds to a curve which falls between the SES activities and noise curves; it also implies that both the SES activities and the noises are not likely to have been produced randomly by a uniform distribution. This can also be seen from Monte Carlo simulations for values of N comparable to those of the experimental signals. Such simulations suggest a low probability to obtain normalized power spectra lying in the region of the SES activities or of the noises.

Furthermore, note that the noises depicted in Fig. 2 (main text) can be described by appropriate values of p_k.

II. The normalised «natural» power spectrum $\Pi(\varphi)$ for SES activities

According to the model of piezo-stimulated acurrents (*6*) a (re)orientation of the electric dipoles occurs when approaching a critical pressure, P_{cr}, obeying the condition:

$$\left(\frac{dP}{dt}\right)_T \frac{v^m}{kT} = -\frac{1}{\tau(P_{cr})} \qquad [A.10]$$

where v^m is the migration volume, defined as

$$v^{m,b} = \left(\frac{\partial g^m}{\partial P}\right)_T$$

g^m being the Gibbs migration energy and $\tau(P_{cr})$ the relaxation time for the (re)orientation process. The values of v^m associated with SES generation should exceed the mean atomic volume by orders of magnitude, and this entails that the relevant (re)orientation process should involve the motion of a large number of «atoms» [see p. 404 of Ref. *6*]. Recent experimental findings (*4*) are consistent with such a «cooperativity». These experiments howed, as mentioned in the main text, that, when approaching the glass transition, the emitted electrical signals have the form of a «Random Telegraph Signal» (RTS). The analysis of the RTS kinetics (*4*) enables one to extract distributions of durations from individual RTS series with two dominant levels. We recall that for a thermally activated two-state process, the time-durations t should be exponentially distributed with a probability density function (pdf): $(1/\tau)$ $\exp(-t/\tau)$. However, Russel and Israeloff (*4*) found that, for all the RTS they studied, the distributions of durations could be well fitted with a stretched exponential or Kohlrausch-Williams-Watt (KWW) law: $\exp[-(t/\tau)^{\beta}]$ with $0.4 < \beta < 0.6$ (cf. it is not generally obeyed for the SES activities reported in this study). This stretching could have arisen from discrete modulation of the rates of an underlying exponential process. Actually some RTS distributions appeared to be exponential in selected shorter sections (4). An alternative derivation of the KWW law, under certain conditions and without any necessity of modulating the rate $1/\tau$, lies in the very stochastic nature of the relaxation process [see p. 350 of Ref. 13, and references therein]. Such a stochastic analysis was based on the concept of clusters, the structural rearrangement of which develops in time. According to this analysis the exponential relaxation of the polarisation is arrested at a random time variable η_i and the instantaneous orientation reached at this instant is «frozen» at a value $\exp(-\beta_i\eta_i)$ where $\beta_i = b = \text{constant}$ (see Fig. 11.19 of Ref. 13).

Assuming that η_i itself follows an exponential distribution, with a time constant $\tau_0 << \tau \approx \tau(P_{cr})$, an almost constant current would be expected for as long as this unit «lives» (i.e., for a duration η_i). The RTS feature of an SES activity might be understood in the following context: The duration Q of a

pulse is just the sum of n such indentical units $Q = \sum_{i=1}^{n} \eta_i$. Under this assumption, the duration Q_k of the k^{th} pulse, in an SES-activity, follows the gamma distribution with a mean lifetime $n_k\tau_0$ and variance $n_k\tau_0^2$ [e.g., see lemma 8.1.6.5. of the NIST-SEMATECH *Engineering Statistics Handbook*, available on-line from www.itl.nist.gov/div898/handbook]; here n_k is the number of exponential lifetime backup units that act cooperatively. Thus, we have

$$\langle Q_k \rangle = \int Q_k \; dp_k \; = n_k \; \tau_0 \qquad [A.11]$$

and

$$\langle Q_k^2 \rangle = \int Q_k^2 dp_k = n_k \, \tau_0^2 + n_k^2 \, \tau_0^2 \qquad [A.12]$$

where dp_k denotes the integral over the pdf of gamma distribution. We have already mentioned that the SES activity is emitted when approaching criticality in the focal area. If at the critical point, n_k backup units were available at the k-th current emission, then the average number of back up units for the $k + 1$ emission would be the same. This assumption is reminiscent of the suggestion that the reorientation of a spin, in the random-field Ising Hamiltonian, will cause on average one more spin to flip at the critical point (*14*, *15*). Under this assumption, Eqs. (A.11) and (A.12) become

$$\langle Q_k \rangle = \int Q_k dp_k = Q_{k-1} \qquad [A.13]$$

and

$$\langle Q_k^2 \rangle = \int Q_k^2 dp_k = \; Q_{k-1}\tau_0 + Q_{k-1}^2 \qquad [A.14]$$

Thus, the time evolution of an SES activity solely depends on the number of the initial backup units, n_1, that were available for the emission of the first pulse of the activity. Bearing this in mind, we now turn to the evaluation of the power spectrum, $P(\omega)$, averaged over all SES activities due to a given value of n_1 and also over all n_1, using the concept of natural time.

$$P(\omega) = \int_0^1 G(\delta)\cos(\omega\delta)d\delta \qquad [A.15]$$

$G(\delta)$ is the average over all n_1 of the time-time correlation function for natural time difference δ

$$G(\delta) = \int\int\int_{0}^{1-\delta} \langle Q_\chi Q_{\chi+\delta}\rangle_{n_1,N} d\chi dP_{N/n_1} dP_{n_1} \qquad [A.16]$$

where the integration $\int dP_{n_1}$ is over the probability for observing an SES activity with n_1 initial backup units for the first pulse. In the inhomogeneous solid earth crust, we intuitively expect that this probability depends on specific inhomogeneities of the system and on the time evolution of pressure reaching P_{cr}. The integration $\int dP_{N/n_1}$ is over the conditional probability to observe an SES activity constituted of N pulses, given that the number of backup units for the first pulse is n_1. For such SES activities, according to the definition of natural time $\chi = k/N$, $N \equiv N(n_1)$ being the number of pulses that were emitted before the cessation of the activity; we thus have the following N-dimensional integral

$$\langle Q_\chi Q_{\chi+\delta}\rangle_{n_1,N} = \langle Q_k Q_{k+N\delta}\rangle_{n_1,N} = \int Q_k Q_{k+N\delta} dp_1 ... dp_k ... dp_{k+N\delta} dp_{k+N\delta+1} ... dp_N \qquad [A.17]$$

where $\int dp_n$ is the integral over the pdf of the gamma distribution that determines the n-th pulse. Using the normalisation of the pdf, we can integrate between $n = k + N\delta + 1$ and N; In this way, Eq. (A.17) simplifies to

$$\langle Q_\chi Q_{\chi+\delta}\rangle_{n_1,N} = \langle Q_k Q_{k+N\delta}\rangle_{n_1,N} = \int Q_k Q_{k+N\delta} dp_1 ... dp_k ... dp_{k+N\delta} \qquad [A.18]$$

Using Eq. (A.13), we now integrate over the probability density functions between $n = k + N\delta$ and $n = k$, to obtain

$$\langle Q_\chi Q_{\chi+\delta}\rangle_{n_1,N} = \langle Q_k Q_{k+N\delta}\rangle_{n_1,N} = \int Q_k^2 dp_1 ... dp_k \qquad [A.19]$$

Considering Eq. (A.14), we derive the one-dimensional integral,

$$\langle Q_\chi Q_{\chi+\delta}\rangle_{n_1,N} = \langle Q_k Q_{k+N\delta}\rangle_{n_1,N} = \int [Q_1^2 + (k-1)\tau_0 Q_1] dp_1 \qquad [A.20]$$

We note that everything depends on the distribution of the first pulse of the SES activity.

Furthermore,

$$\langle Q_\chi Q_{\chi+\delta}\rangle_{n_1,N} = \langle Q_k Q_{k+N\delta}\rangle_{n_1,N} = k\tau_0^2 n_1 + \tau_0^2 n_1^2 = \chi\tau_0^2 n_1 N + \tau_0^2 n_1^2, \quad [A.21]$$

Integrating Eq. (A.16) over χ in Eq. (A.16), we have

$$G(\delta) = \tau_0^2\left[\frac{(1-\delta)^2}{2}\left(\int\int n_1 N dP_{N/n_1} dP_{n_1}\right) + (1-\delta)\left(\int\int n_1^2 dP_{N/n_1} dP_{n_1}\right)\right]. \quad [A.22]$$

The number N of the pulses of the SES activities is expected to scale proportionally with n_1, and thus we define

$$p_0 = \frac{\int n_1^2 dP_{N/n_1}\, dP_{n_1}}{\int n_1 N dP_{N/n_1}\, dP_{n_1}} \quad [A.23]$$

Inserting (A.23) into Eq. (A.22), we find

$$G(\delta) \propto \left(\frac{(1-\delta)^2}{2} + p_0\,(1-\delta)\right) \quad [A.24]$$

It is seen that the right-hand side of Eq. (A.24) is independent of n_1; thus, if the limit we want to evaluate actually exists, it should obey the condition $G(0) = 1$. Note that the analysis in the natural time for the same SES activity with different sampling rates —and thus different $N(n_1)$— leads to approximately the same normalized power spectrum curve. Therefore, the aforementioned limit becomes meaningful. The condition $G(0) = 1$ implies that $p_0 = 0.5$. Performing now the integration in Eq. (A.15) we find

$$P(\omega) \propto \frac{3}{2\omega^2} - \frac{\cos\omega}{2\omega^2} - \frac{\sin\omega}{\omega^3} \quad [A.25]$$

which leads to the normalized power spectrum

$$\Pi(\omega) = \frac{18}{5\omega^2} - \frac{6\cos\omega}{5\omega^2} - \frac{12\sin\omega}{5\omega^2} \qquad [A.26]$$

Expanding Eq. (A.26) around $\omega = 0$

$$\Pi(\omega) = 1 - 0.07\omega^2 + \ldots \qquad [A.27]$$

which implies that

$$\varkappa_1 = <\chi^2> - <\chi>^2 = 0\ 07. \qquad [A.28]$$

The experimental results, when read in the natural time domain, are shown in Figs. A1 and A2a for the SES activities and earthquakes (EQ)s respectively. For the region of natural frequencies $0< \phi <0.5$, where $\Pi(\phi)$ should be considered as a characteristic function for $p(\chi)$ (see main text). The experimental results agree favourably as seen in Figs. A2b,c and A3, for EQs and SES activities, respectively, with the theoretical estimations of Eqs. (A.26).

We must clarify that the said theoretical lines were developed for the SES activities only. The fact that the seismicity natural spectrum falls (in the region $0< \phi <0.5$) a few days before the main shock on that of the preceding SES activity (Fig. A4; this cannot be attributed to chance, see Table A5) might indicate that Eq. (A.26) is a good approximation (Fig. A2b) for the seismic events as well. This point, however, merits further investigation (see also below).

III. The normalized «natural» power spectrum for seismicity

The seismic moment M_0 was estimated using the relation $\log_{10}(M_0) = 1.64ML + \text{const.}$ (*16*) The values of the local magnitude ML were taken from the catalogue of National Observatory of Athens (NOA), available from www.gein.noa.gr on Oct. 17 2001). The data for the EQs that preceded the main shocks labeled K, E, S and A are given in Tables A1-A4.

In order to further investigate the aforementioned point concerning the appropriateness of Eq. (A.26) to describe the evolution of seismicity, we proceeded to the following analysis: all the seismic data, available from NOA, were analysed in the natural time domain, since 1966 until the main shock

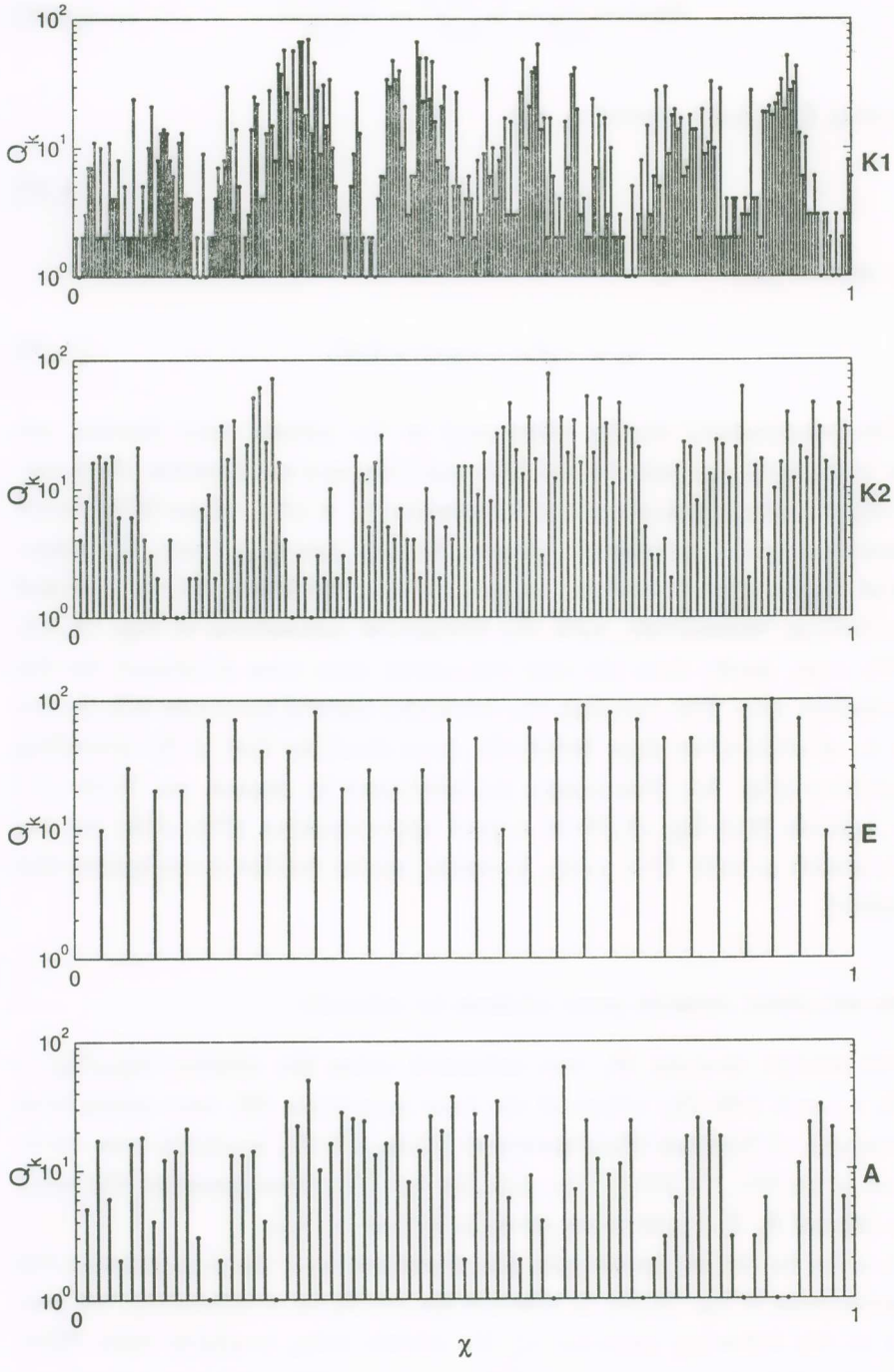

Fig. A1. How the SES activities depicted in Fig. 1 (main text) are read in «natural time».

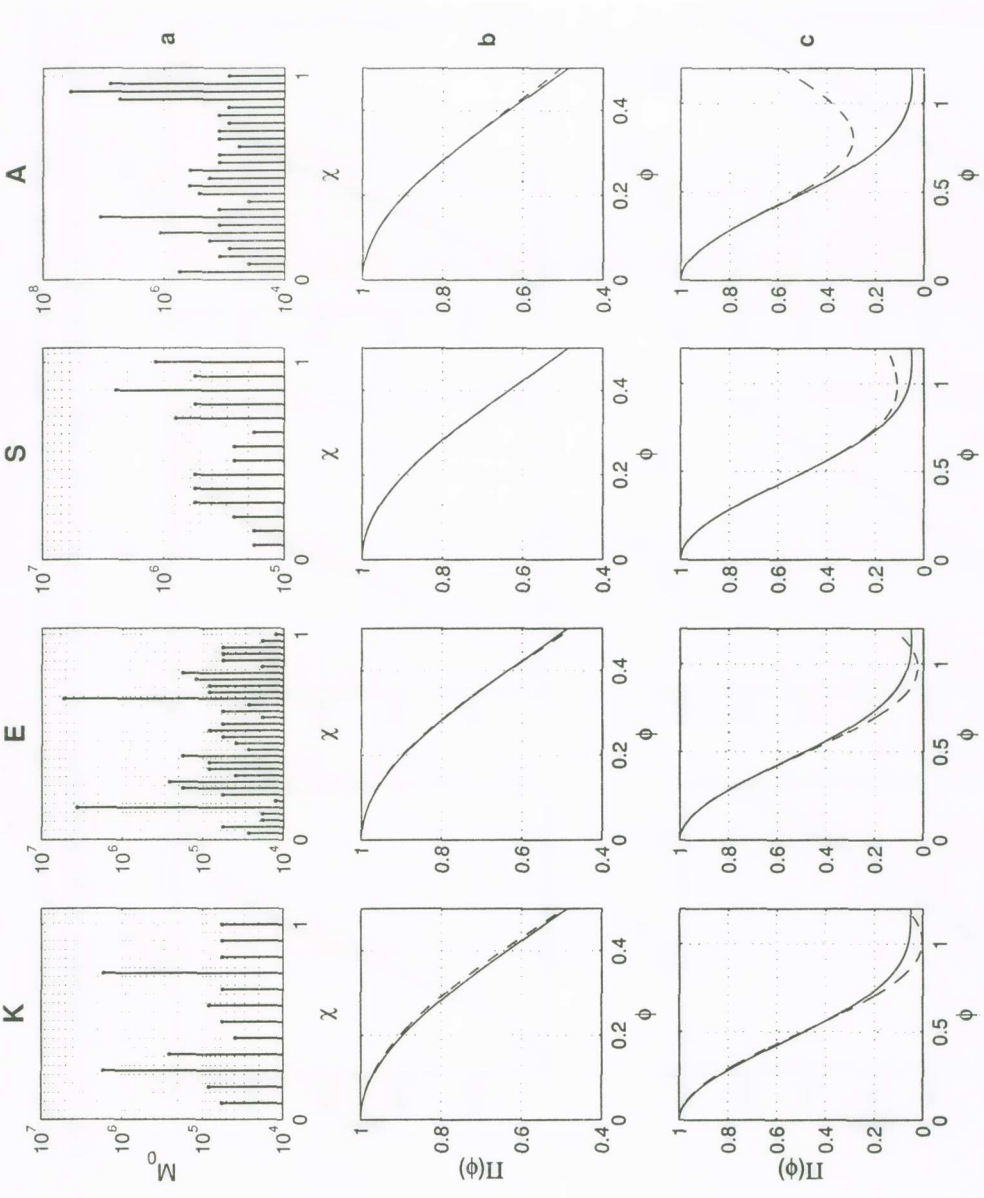

Fig. A2. (a) How the EQs that preceded the main shocks K, E, S and A (see Tables 1A to 4A) are read in «natural time» (b), (c): comparison of the normalised power spectra Π(ϕ) for EQs in (a) (broken lines) with those predicted from Eq. (A. 26) (solid lines). Note that (b) refers to the range $0 < \phi \leq 0.5$, while (c) to $0 < \phi \leq 1.2$.

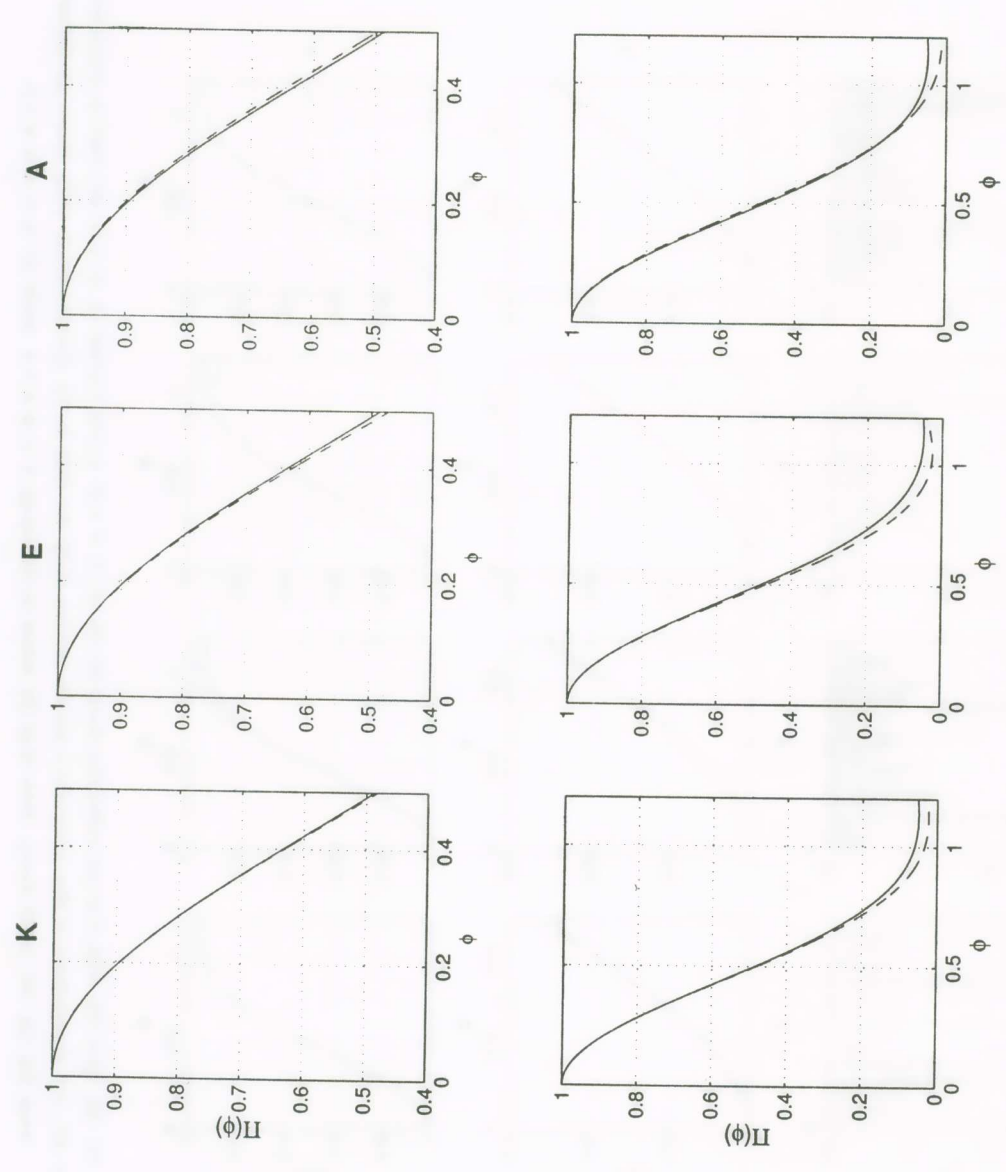

Fig. A3. Comparison of the normalised power spectra $\Pi(\phi)$ for the SES activities that preceded the EQs labeled K, E and A (broken lines) with those estimated from the theoretical aspects (Eq. (A.26), solid lines). Upper: ϕ lying between 0 and 0.5; bottom: $0 < \phi \leqslant 1.2$.

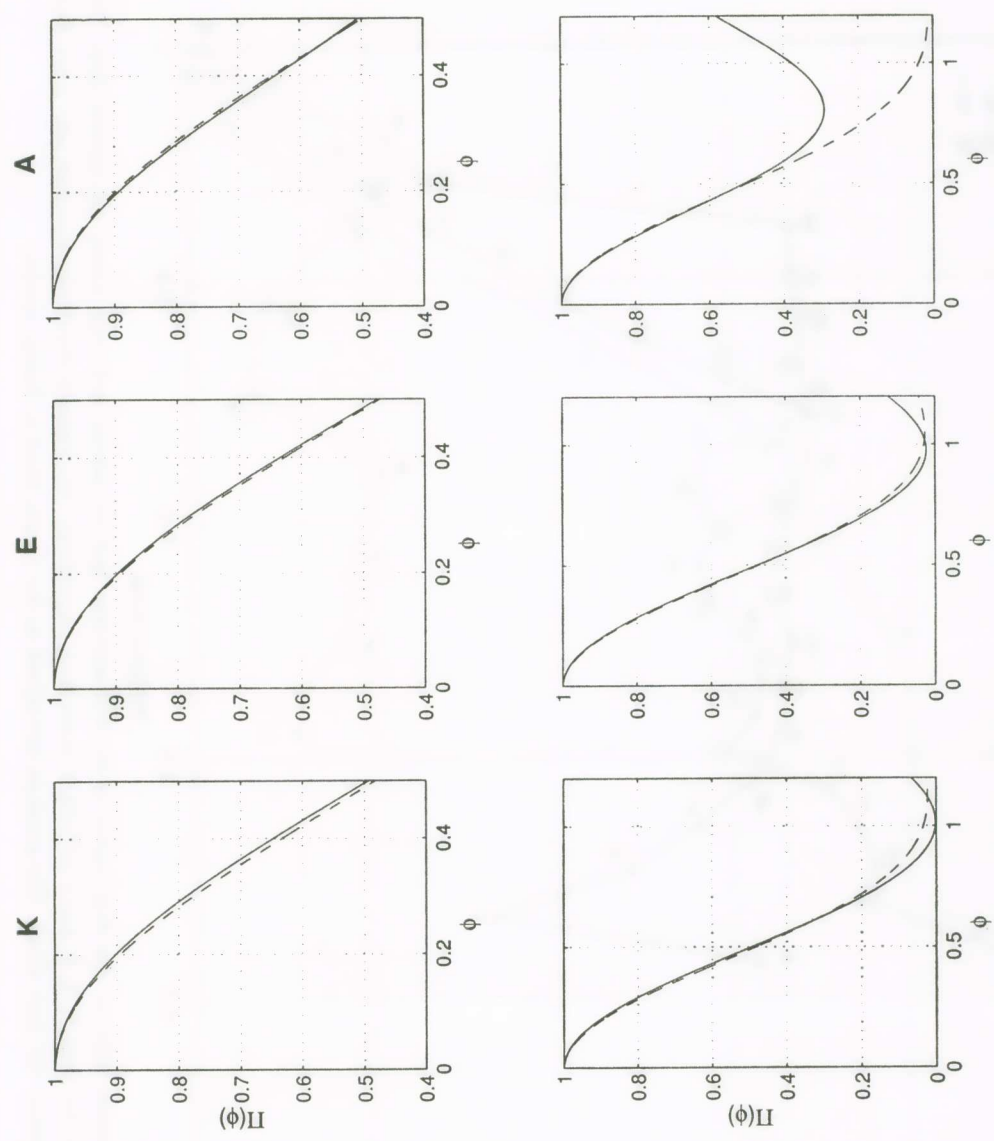

Fig. A4. Comparison of the normalised power spectra Π(ϕ) for the SES activities given in Fig. 1 (main text) with the corresponding spectra of the EQs given in Fig. A2 b, c. Broken lines correspond to the SES activities while the solid lines to the EQs .

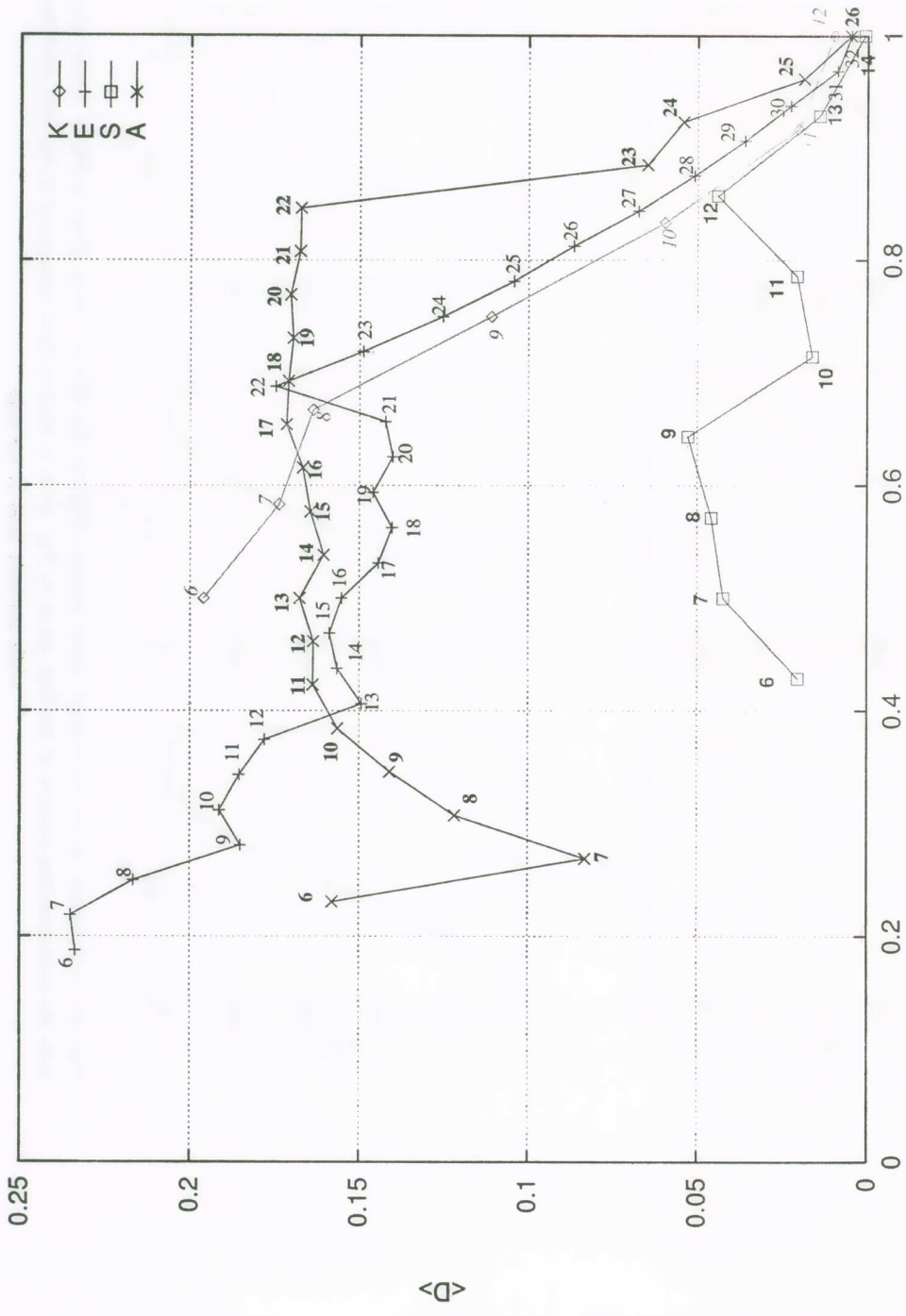

Fig. A5. The average distance between the $\Pi(\phi)$ curves of the SES activities and the seismic activities versus the natural time. The various lines correspond to the cases K, E, S, and A of Table 1 (main text) respectively. The distance drastically decreases only a few days before the main shock. The numbers correspond to the events listed in Tables A1-A4.

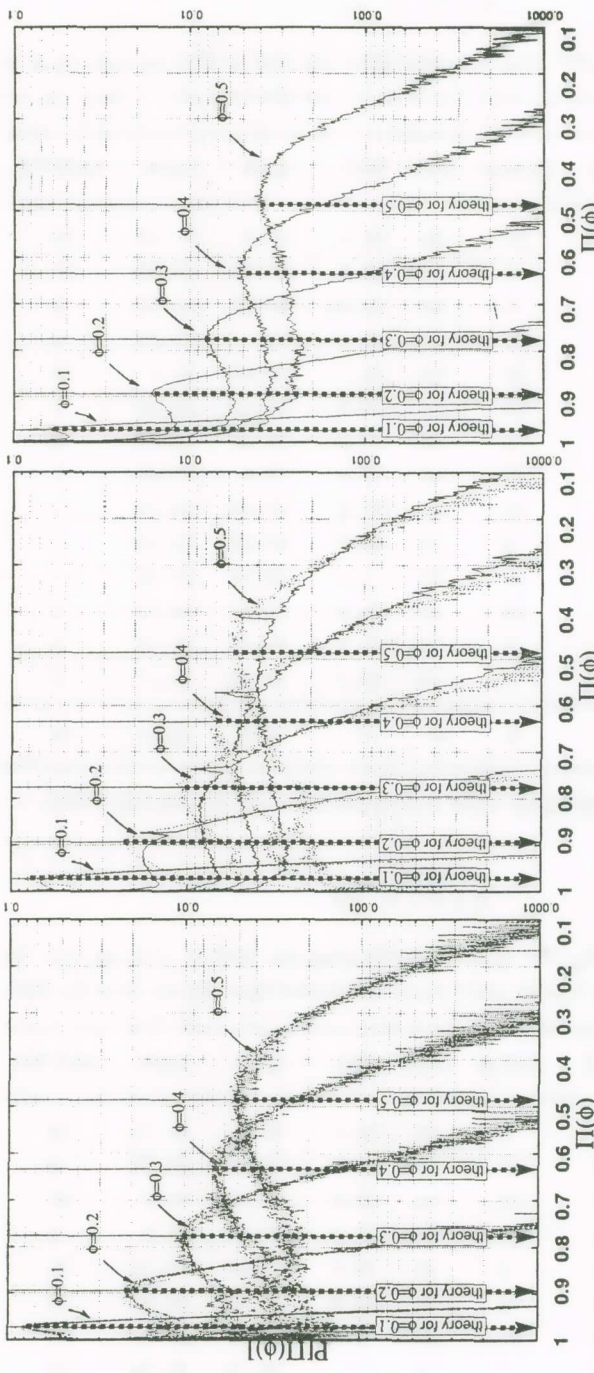

Fig. A6. The observed probability P[Π(φ)] to obtain a given value of Π(φ) versus the normalized «natural» power spectra Π(φ) for the seismicity: (a) during the period since 1966 until the main shock under discussion, for each of the four regions mentioned in Tables A1-A4, (b) for the whole Greek area during the period 1966-2001 (the solid lines are calculated without any magnitude threshold, while the dotted ones correspond to the EQs with ML ≥ 4.3). When the magnitude was not reported the value $ML_{\sqcup}$=2.0 was assumed. In curve (c), the case of the San Andreas fault system is depicted: using the USGS catalogue, available from *http://neic.usgs.gov/neis/epic/epic.html*, for the period 1973-2001, within the area $N_{31}^{42}W_{125}^{114}$. (The moment magnitude relations available from Global Seismological Services at the site. http://www.seismo.com/msop/nmsop/03%20source/source6/source6.html, were considered for the different magnitude scales reported in this catalogue).

TABLE A1.

All EQS within $N_{39\cdot2}^{40\cdot5}$ $E_{20\cdot3}^{22\cdot0}$ that occurred after the SES at IOA on Apr. 18 & 19, 1995 until the 6.6 (Ms from USGS) main shock at Kozani-Grevena (K) on May 13, 1995.

NR	YEAR	MON	DAY	HOUR	MIN	SEC	LAT.	LON.	DEPTH	ML
1	1995	4	27	15	16	55.3	39.5	21.13	10	2.9
2	1995	4	30	6	58	24.8	39.79	20.72	29	3
3	1995	4	30	7	50	32.14	40.44	21.85	3	3.8*
4	1995	4	30	21	12	42.6	40	20.66	5	3.3
5	1995	4	30	23	24	54.7	39.81	20.5	10	2.8
6	1995	4	30	23	46	42.5	39.58	20.58	5	2.9
7	1995	5	1	1	49	55.5	39.89	20.74	5	3
8	1995	5	1	22	47	21.1	39.9	21.01	5	2.9
9	1995	5	2	15	52	18.6	39.55	20.58	5	3.8
10	1995	5	7	5	19	50.3	40.12	20.52	5	2.9
11	1995	5	10	15	23	2.4	39.28	21.69	10	2.9
12	1995	5	10	18	24	56.3	39.91	20.72	5	2.9
13	1995	5	13	8	42	12.3	40.07	21.75	5	3.7
14	1995	5	13	8	43	18.7	40.02	21.77	5	4
EO	**1995**	**5**	**13**	**8**	**47**	**17**	**40.18**	**21.71**	**39**	**6.1**

* This event is not reported by NOA but comes from USGS with ML(THE).

TABLE A2.

All* EQs within $N_{37\cdot5}^{39\cdot7}$ $E_{21\cdot5}^{25\cdot0}$ that occurred after the SES at VOL on Apr. 30, 1995 until the 6.5(Ms from USGS) main shock at Eratini-Egio (E) on June 15, 1995.

NR	YEAR	MON	DAY	HOUR	MIN	SEC	LAT.	LON.	DEPTH	ML
1	1995	5	2	8	26	56.1	38.2	21.76	32	2.7
2	1995	5	4	16	11	49	38.33	22.05	5	2.9
3	1995	5	6	17	44	59.5	38.51	21.5	24	2.6
4	1995	5	6	23	10	21.4	38.44	21.8	5	2.6
5	1995	5	8	5	11	9.1	38.32	22.14	21	4
6	1995	5	9	12	48	34.8	38.32	22.09	10	2.5
7	1995	5	10	15	23	2.4	39.28	21.69	10	2.9
*	1995	5	12	7	25	13	39.12	24.48	31	3.6
8	1995	5	13	11	53	1.1	39.56	22.53	10	3.2

9	1995	5	13	13	31	55.2	38.52	22.04	5	3.3
10	1995	5	15	20	15	13.4	38.13	21.66	9	2.8
*	1995	5	16	5	15	44.5	38.97	23.18	33	3.6
11	1995	5	16	10	1	30.6	38.93	21.77	5	3
12	1995	5	17	23	10	52.7	39.7	21.91	5	3
13	1995	5	18	4	48	27.8	38.3	22.18	22	3.2
14	1995	5	19	23	19	49.2	38.24	21.87	11	2.7
15	1995	5	19	23	59	26.6	38.12	22.65	34	2.8
16	1995	5	20	20	32	33.3	38.41	21.79	9	2.9
17	1995	5	22	17	35	27.2	39.54	22.43	5	3
18	1995	5	25	16	41	31.4	39.08	23.5	10	2.9
19	1995	5	26	1	28	47.3	38.36	22.63	10	2.6
20	1995	5	26	7	9	25.1	38.36	22	5	2.9
21	1995	5	26	21	30	35.5	38.43	21.81	6	2.7
22	1995	5	28	19	56	41	38.38	21.96	5	4.1
23	1995	5	28	20	9	14.7	38.4	21.9	5	3
24	1995	5	28	21	51	1.6	38.28	22.67	10	3
*	1995	5	29	13	3	3.7	37.61	22.78	5	2.8
25	1995	5	30	9	6	31.6	38.5	21.74	5	3.1
*	1995	5	31	12	25	42.5	39.21	22.88	10	3
*	1995	5	31	21	43	30.7	39.39	22.63	29	3
26	1995	6	1	14	4	53.5	38.13	21.74	5	3.2
*	1995	6	2	14	47	46.8	39.2	23.14	32	3.1
27	1995	6	4	18	47	35.5	38.5	22.25	5	2.6
28	1995	6	5	15	4	40.6	38.88	21.51	5	2.9
29	1995	6	6	20	12	14.5	38.8	21.58	5	2.9
30	1995	6	12	20	27	7.2	38.21	22.22	39	2.9
31	1995	6	13	2	48	39.8	38.29	22.47	10	2.6
32	1995	6	14	11	8	41.6	38.04	21.54	28	2.5
EO	**1995**	**6**	**15**	**0**	**15**	**51**	**38.37**	**22.15**	**26**	**5.6**

* Excluding those close to VOL and inside the Peloponese, as stated in the prediction text (*2*).

TABLE A3.

All EQS between $N_{37.0}^{38.5}$ $E_{20.3}^{21.7}$ that occurred after the SES at IOA on Oct. 10, 1997 until the 6.4 (Ms from USGS) main shock at Strofades (S) on Nov. 18, 1997.

NR	YEAR	MON	DAY	HOUR	MIN	SEC	LAT.	LON.	DEPTH	ML
*	1997	10	3	2	51	25.6	37.52	21.26	5	3

1	1997	10	3	23	3	50.6	37.6	21.23	10	3.2
*	1997	10	8	0	0	41.6	37.89	21.25	8	2.7
2	1997	10	9	2	34	46.8	37.34	20.73	5	3.2
*	1997	10	9	9	27	28.8	37.99	21.4	10	2.8
*	1997	10	10	3	31	13.1	38.11	20.56	5	3
3	1997	10	11	23	1	41.6	37.8	21.29	5	3.3
4	1997	10	13	23	12	19.2	37.44	20.73	5	3.5
*	1997	10	17	19	47	36.9	37.1	21.49	5	2.9
*	1997	10	18	2	56	25.4	37.41	20.78	10	2.7
*	1997	10	18	5	49	34.4	37.37	21.62	10	2.8
*	1997	10	18	5	52	57	37.81	21.1	10	2.9
*	1997	10	18	22	39	5.1	38.26	21.56	10	2.5
*	1997	10	19	0	13	33.2	38.34	21.66	5	2.7
*	1997	10	19	12	29	9.7	37.56	20.79	23	2.8
*	1997	10	20	17	29	31.5	37.67	21.18	5	2.8
*	1997	10	20	20	26	24	37.6	21.28	5	2.8
*	1997	10	22	11	3	49.4	37.56	21.27	5	2.9
*	1997	10	24	2	18	52.3	37.49	21.14	30	2.7
*	1997	10	24	10	24	58	37.53	21.24	15	2.8
5	1997	10	27	1	29	33.4	37.44	20.7	5	3.5
*	1997	10	31	11	46	10.3	38.34	20.46	25	3.1
6	1997	11	1	6	8	15.5	37.68	21.4	5	3.5
7	1997	11	1	8	33	28.6	37.65	21.36	5	3.3
*	1997	11	1	20	27	37.5	37.62	21.28	10	2.7
*	1997	11	1	20	31	42.5	37.62	21.48	10	2.8
*	1997	11	3	0	42	16.9	37.6	21.33	5	2.9
*	1997	11	3	8	29	33	37.47	21.45	31	3
*	1997	11	3	17	56	43.9	37.5	21.25	27	2.8
*	1997	11	4	17	10	13.5	37.58	21.32	10	2.9
*	1997	11	4	19	56	59.7	37.62	21.55	10	2.6
8	1997	11	4	21	24	44.2	37.54	21.26	5	3.3
*	1997	11	6	19	38	7.8	37.66	21.36	5	3
*	1997	11	6	20	29	19.9	37.19	20.63	5	2.9
9	1997	11	8	4	31	30.4	37.68	21.51	5	3.2
10	1997	11	10	0	55	8.7	37.91	20.69	5	3.6
*	1997	11	11	4	6	48.3	37.05	20.81	5	2.9
*	1997	11	12	4	37	12.4	37.78	21.12	10	3
11	1997	11	12	11	19	23.6	37.93	20.89	5	3.5
*	1997	11	13	1	35	55.8	37.68	21.35	5	2.8
12	1997	11	13	10	30	17.2	36.99	21.5	5	3.9
13	1997	11	16	18	38	51.6	37.2	20.33	10	3.5
14	1997	11	17	6	58	9.8	37.61	21.42	22	3.7

*	1997	11	17	22	51	26.8	37.61	21.34	5	3
EO	**1997**	**11**	**18**	**13**	**7**	**36.9**	**37.26**	**20.49**	**5**	**6.1**

* Only EQs with ML $\geqslant$ 3.2 were included in the calculations.

TABLE A4.

All* EQS within $N_{38\cdot7}{}^{39\cdot5}$ $E_{22\cdot0}{}^{25\cdot0}$ that occurred after the SES at VOL on Mar. 17, 2001 until the 6.6 (Ms from USGS) main shock in Aegean sea (A) on July 26, 2001.

NR	YEAR	MON	DAY	HOUR	MIN	SEC	LAT.	LON.	DEPTH	ML
1	2001	3	23	23	13	43.3	38.74	23.6	5	3.5
2	2001	3	25	11	29	24.9	38.85	23.43	10	2.8
3	2001	4	13	21	24	2.5	39.09	23.45	5	3.1
4	2001	4	16	3	27	41	39.11	22.46	5	3
5	2001	4	24	11	39	9.7	39.19	22.71	10	3.2
6	2001	5	14	8	33	6.1	38.79	23.68	4	3.7
7	2001	5	14	17	26	3.9	38.98	23.19	6	3.1
8	2001	5	19	3	11	16.1	39.16	22.57	5	4.3
9	2001	5	20	1	36	21.4	39.49	22.55	37	3.1
*	2001	5	20	3	37	46	38.85	22.01	5	3.5
10	2001	5	23	1	24	10.7	38.74	23.84	10	2.8
11	2001	5	25	22	23	21	38.83	24.85	10	3.3
12	2001	5	27	0	46	38.2	38.83	24.71	27	3.4
13	2001	5	30	7	37	58.9	38.88	23.68	5	3.2
14	2001	6	8	23	40	37.3	39.08	23.17	5	3.4
15	2001	6	9	2	1	17.3	39.33	23.07	2	3.1
16	2001	6	20	6	34	5.5	38.86	23.3	21	3.1
17	2001	7	4	19	57	43.9	39.48	22.23	5	2.9
*	2001	7	5	2	49	16.6	39.08	22	5	2.9
18	2001	7	10	22	26	49.5	39.36	23.02	10	3.1
19	2001	7	12	1	49	9	39.32	22.96	5	3.1
20	2001	7	12	3	2	40.7	39.34	23.57	13	3
21	2001	7	13	1	52	55.8	39.31	23.07	5	3.1
22	2001	7	19	20	11	19	39.31	23.42	37	3
23	2001	7	21	12	45	59.8	39.1	24.35	21	4.1
24	2001	7	21	12	47	38.7	39.06	24.35	18	4.6
25	2001	7	25	15	43	13.4	39.06	24.32	19	4.2
26	2001	7	25	16	35	40.6	39.04	24.19	5	3
EO	**2001**	**7**	**26**	**0**	**21**	**39.3**	**39.05**	**24.35**	**19**	**5.3**

* Excluding those outside the predicted area (see ref. *12*).

TABLE A5.

The estimated probability P to achieve the behavior depicted in Fig. 3 by chance.

General Conditions	Case	Minimum of D between the:	P%*
a) The difference D (see Fig. A5) ≤ 0.0095	K	11th and 12th event	$< 3.5 \pm 0.8$
b) Continuous decrease of D in the last three events	E	30th and 32th event	$< 1.9 \pm 0.2$
c) The seismic spectrum approaches the theoretical curve, Eq. (A.26), from below	S	12th and 14th event	$< 1.6 \pm 0.2$
d) D becomes minimum a few days only before the main shock, see the 3rd column	A	25th and 26th event	$< 1.3 \pm 0.2$

* Value resulting from continuous scanning of the EQ catalogue, since 1966 until the main event in each case. The calculation was made in each of the four regions mentioned in Tables A1-A4.

under discussion, for each of the regions mentioned in the Tables A1-A4 (Fig. A6a); this was repeated for the whole Greek region, during the period 1966-2001 (Fig. A6b). The calculation was made in each case by considering a number of subsequent events, from 6 to 40 (i.e., around the limits in the number of the EQs used in the curves depicted in Fig. A2 b, c), and scanning the whole catalogue. An inspection of Fig. A6a reveals that the local maxima of the curves, each one of which was drawn for a certain ϕ-value, for each of the aforementioned four regions, correspond to $\Pi(\phi)$ values that lie very close to those predicted from Eq.(A.26). The larger deviations were observed in the case K. As for Fig. A6b, it indicates that, when considering the totality of the events (solid lines), such an agreement is not evident; on the other hand, when selecting a considerable threshold, e. g., ML $\geq$ 4.3, an agreement between the $\Pi(\phi)$ values, corresponding to the maxima of the curves, and those predicted form Eq. (A.26) becomes apparent. We note that this agreement holds for other seismic areas as well, e.g., if we consider the seismic data for the San

Andreas fault system (Fig. A6c). The same curves are practically obtained if the number of subsequent events is changed, e.g., within the limits 6-100. (c.f., the slight differences between Fig. A6b and Fig. A6c might be associated with the different b-values in the usual Gutenberg — Righter relation, log $N = a-b\ M$, in the two areas studied).

By ending this paper we clarify that in a separate study (17) we have applied the rescaled range Hurst and detrended fluctuation analyses to the electric signals that precede rupture; these lead to power-law exponents which are consistent with the existence of long-range correlations (memory). Furthermore, the quantity $\varkappa_1$ (see Eq A.2) was found to be related to the generalised Hurst exponent h(2), when the latter is calculated in the "natural" time domain.

Remark. By changing the sampling rate (i.e., re-sampling the data), in the range 1 sample/sec to 1 sample/20 sec (see the example of E), we have found that $\varkappa_1$ is *scale invariant* for the SES activities, while for the artificial noises is not. The latter exhibit a decrease of $\varkappa_1$ when the sampling rate decreases (i.e., the scale increases), and at the larger scales (i.e., 1 sample/10sec to 1 sample/20 sec) have $\varkappa_1$-values which tend to the value of the uniform distribution $1/12 = 0.0833$.

Note added in the proofs: Studying the function $F_q = <x^q> - <x>^q$, the signals are again classified in the range $q \in (1,2]$. The derivative dF_q/dq, at $q \to 1$, i.e., the quantity $<x\ln x> - <x><\ln x>$, is reminiscent of an «entropy» (which is also found to differentiate human heart recordings, ECG, when comparing healthy — and non healthy — or «sudden death» — individuals). This quantity again provides a classification of the signals having larger values for the artificial noises and lower for the SES activities (while its value ≈ 0.0966 for the «uniform» distribution lies just in the border between them). The value of $\varkappa_1$ (i.e., the value of F_q for $q = 2$) is proportional to this «entropy» and hence we may say the following: A «uniform distribution» lies just in the boundary between the SES activities (critical dynamics and hence strongly correlated signals, scale invariant entropy) and «artificial» noises (correlated signals, but to a smaller extent than SES, exhibiting scaling dynamics characteristic of complex systems, but having non-scale invariant «entropy»).

ΠΕΡΙΛΗΨΗ

Προτάσεις χωρο-χρονικῆς πολυπλοκότητας γιὰ τὴν συσχέτιση μεταξὺ Σεισμικῶν Ἠλεκτρικῶν Σημάτων καὶ Σεισμικότητας.

Τὰ Σεισμικὰ Ἠλεκτρικὰ Σήματα (SES) εἶναι χαμηλῆς συχνότητας (≤ 1Hz) μεταβολὲς τοῦ ἠλεκτρικοῦ (Ε) πεδίου τῆς Γῆς τὰ ὁποῖα ἔχουν ἀνιχνευθεῖ στὴν Ἑλλάδα (1, 2) καὶ στὴν Ἰαπωνία (3) καὶ ἔχουν βρεθεῖ νὰ προηγοῦνται τῶν σεισμῶν σὲ χρόνους ποὺ κυμαίνονται ἀπὸ ἀρκετὲς ὧρες ἕως μερικοὺς μῆνες. Ἡ ἀνάλυση αὐτῶν τῶν σημάτων μπορεῖ νὰ ὁδηγήσει καὶ στὸν προσδιορισμὸ τῆς ἐπικεντρικῆς περιοχῆς. Στὴν παροῦσα ἐργασία δείχνουμε ὅτι τὸ φασματικὸ περιεχόμενο τῆς σεισμικότητας τῆς «ὑποψήφιας» γιὰ σεισμικὴ διέγερση περιοχῆς συμπίπτει τελικῶς μὲ τὸ φασματικὸ περιεχόμενο τῆς δραστηριότητας τῶν SES λίγο πρὶν ἀπὸ τὸν κύριο σεισμό. Τὸ κύριο σημεῖο εἶναι ὅτι καὶ τὰ δύο φάσματα πρέπει νὰ ὑπολογιστοῦν σὲ ἕνα νέο χρόνο, ποὺ ὀνομάζεται «φυσικὸς χρόνος», καὶ μετρᾶται ἀπὸ τὴν στιγμὴ καταγραφῆς τοῦ SES. Συνεπῶς, ἀπὸ τὴν στιγμὴ ποὺ τὸ φασματικὸ περιεχόμενο τῶν SES εἶναι ἐκ τῶν προτέρων γνωστό, ἡ συνεχὴς παρακολούθηση τοῦ φάσματος τῆς ἐξελισσόμενης σεισμικότητας θὰ μποροῦσε νὰ ὁδηγήσει στὸν ὑπολογισμὸ τοῦ χρόνου γένεσης τοῦ κυρίως σεισμοῦ μὲ ἀκρίβεια τῆς τάξης τῶν μερικῶν ἡμερῶν.

REFERENCES

1. P. Varotsos, K. Alexopoulos, K. Nomicos, M. Lazaridou, *Nature* **322**, 120 (1986).
2. P. Varotsos et al., in *The Critical Review of VAN: Earthquake Prediction from Seismic Electric Signals*, Sir J. Lighthill Ed. (World Scientific, Singapore, 1996) pp. 29-76.
3. S. Uyeda, T. Nagao, Y. Orihara, T. Yamaguchi, I. Takahashi, *Proc. Natl. Acad. Sci USA* **97**, 4561 (2000).
4. E. V. Russell, N. E. Israeloff, *Nature*, **408**, 695 (2000).
5. P. Varotsos, *Acta Geophys. Pol.* **49**, 1 (2001).
6. P. Varotsos, K. Alexopoulos, *Thermodynamics of Point Defects and their Relation with Bulk Properties* (North Holland, Amsterdam, 1986).
7. P. Varotsos, *Physics of Seismic Electric Signals* (TERRAPUB, Tokyo, in press).
8. P. Varotsos, N. Sarlis, E. Skordas, *Proc. Japan Acad.* **77B**, 93 (2001).
9. L. P. Kadanoff, *Statistical Physics, Dynamics and Renormalization* (World Scientific, Singapore 2000).
10. E. Manousakis, R. Salvador, *Phys. Rev.* B, **40**, 2205 (1989).

11. P. Varotsos *et al, Acta Geophys. Polonica*, **46**, 56 (1998).
12. P. Varotsos, N. Sarlis, E. Skordas, *Acta Geophys. Polonica*, **49**, 425 (2001).
13. A. K. Jonscher, *Universal Relaxation Law*, (Chelsea Dielectric Press, London, 1996).
14. M. C. Kuntz, J. P. Sethna, *Phys. Rev. B*, **62**, 11699 (2000).
15. J. P. Sethna, K. A. Dahmen, C. R. Myers, *NATURE*, **410**, 242 (2001).
16. Z. Roumelioti, *Calculation of the focal parameters and strong motion simulation for Western Greece*, (M. Sc. Thesis, University of Thessaloniki, 1999, in Greek).
17. P. Varostos, N. Sarlis, E. Skordas, *Phys. Rev. E* (to be published).